



Kahramanmaraş Sutcu Imam University

Journal of Engineering Sciences



Geliş Tarihi : 13.06.2024
Kabul Tarihi : 08.07.2024

Received Date : 13.06.2024
Accepted Date : 08.07.2024

DIRECT HF ETCHING-DERIVED $Ti_3C_2T_x$: A POTENT ADSORBENT FOR BASIC RED 46 DYE

DOĞRUDAN HF AŞINDIRMA YOLUYLA ELDE EDİLMİŞ $Ti_3C_2T_x$: BASIC RED 46 BOYASI İÇİN GÜÇLÜ BİR ADSORBAN

Yunus AKSOY¹ (ORCID: 0000-0002-6047-2101)

¹ Fırat Üniversitesi, Çevre Mühendisliği Bölümü, Elazığ, Türkiye

*Sorumlu Yazar / Corresponding Author: Yunus AKSOY, yaksoy@firat.edu.tr

ABSTRACT

Dye contamination poses a significant threat to water sources and ecosystems, necessitating the development of efficient treatment methods. Basic Red 46 (BR 46), a highly toxic and persistent azo dye, presents specific challenges in removal from water resources. This study investigates the adsorption efficiency of $Ti_3C_2T_x$ (Titanium Carbide) MXene, synthesized via direct HF (Hydrofluoric acid) etching, for BR 46 removal. The physicochemical properties of $Ti_3C_2T_x$ were characterized using Fourier transform infrared (FTIR) spectroscopy, X-ray diffraction (XRD), and scanning electron microscopy (SEM). Additionally, the effects of pH, MXene amount, and initial BR 46 concentration on BR 46 adsorption were also investigated. The results show a maximum BR 46 removal efficiency of 99.98% at pH 2, 4 g/L $Ti_3C_2T_x$ dose, 50 mg/L BR 46 concentration, and 90 min contact time. This research underscores the potential of $Ti_3C_2T_x$ MXene as a potent adsorbent for BR 46 dye removal, offering insights for future water treatment applications.

Keywords: $Ti_3C_2T_x$, adsorption, Basic Red 46

ÖZET

Boya kirliliği, su kaynakları ve ekosistemler için önemli bir tehdit oluşturmakta ve etkili arıtma yöntemlerinin geliştirilmesini gerektirmektedir. Oldukça toksik ve kalıcı bir azo boyası olan Basic Red 46 (BR 46), su kaynaklarından uzaklaştırılmasında belirli zorluklar ortaya çıkarmaktadır. Bu çalışmada, BR 46 giderimi için doğrudan HF (Hidroflorik asit) aşındırma yoluyla sentezlenen $Ti_3C_2T_x$ (Titanyum Karbür) MXene'nin adsorpsiyon verimliliği araştırılmıştır. $Ti_3C_2T_x$ 'in fizikokimyasal özellikleri, Fourier dönüşümlü kızılötesi (FTIR) spektroskopisi, X-ışını difraktometresi (XRD) ve taramalı elektron mikroskobu (SEM) kullanılarak karakterize edilmiştir. Ayrıca pH, MXene miktarı ve başlangıç BR 46 konsantrasyonunun BR 46 adsorpsiyonu üzerindeki etkileri de araştırılmıştır. Sonuçlar, pH 2'de, 4 g/L $Ti_3C_2T_x$ dozunda, 50 mg/L BR 46 konsantrasyonunda ve 90 dakika temas süresinde %99,98'lik maksimum BR 46 giderim verimliliğini gösterir. Bu araştırma, $Ti_3C_2T_x$ MXene'nin BR 46 boya giderimi için güçlü bir adsorban olarak potansiyelinin altını çizerek gelecekteki su arıtma uygulamaları için öngörüler sunmaktadır.

Anahtar Kelimeler: $Ti_3C_2T_x$, adsorpsiyon, Basic Red 46

INTRODUCTION

Dye contamination in water sources is a significant issue with detrimental effects on ecosystems. Dyes, particularly azo dyes, are widely used in industries such as textiles and contribute to water pollution (Hashemi & Kaykhahi, 2022). The discharge of effluents from dye processing industries contains a variety of pollutants, including color compounds, suspended solids, acids, chlorine dyes, chromium, and phenolic substances (Devasia, Anand, & Nair, 2022). These dyes are persistent and non-biodegradable, leading to long-term hazards in the environment (Maheshwari, Agrawal, & Gupta, 2021). The presence of dyes in water bodies reduces aesthetic value, affects photosynthesis, and disrupts the food chain and web. Dyes can accumulate and biomagnify, causing toxicological impacts on aquatic flora, fauna, and human health. Azo dyes, in particular, are highly toxic and can generate harmful byproducts (Lekhak, 2023). The textile industry alone contributes a significant portion of industrial water pollution. Various physical, chemical, and biological methods are employed for dye removal from wastewater, including advanced oxidation, filtration, and microbial degradation (Ghosh & Sarkar, 2022). Nanotechnology, specifically the use of nanoparticles, shows promise in the effective elimination of dye contaminants (Kamsonlian & Agarwal, 2023). Overall, dye contamination poses a serious threat to water sources and ecosystems, necessitating the development and implementation of efficient treatment methods (Hashemi & Kaykhahi, 2022).

Public awareness and education can play a crucial role in mitigating dye contamination in water sources. By increasing public awareness about the harmful effects of dye pollution and the importance of clean water, individuals can be motivated to take action to prevent and reduce contamination. Educating the public about the sources and consequences of dye pollution can help them make informed choices and adopt sustainable practices in industries that use dyes, such as the textile sector (Mustafa, Jamil, Zhang, & Girmay, 2022).

Regulatory frameworks are in place to monitor and control dye pollution in water. Environmental legislation commonly obligates textile factories to treat dye effluents before discharge into water bodies (Allirani, 2022). Stringent regulations are enforced to minimize the introduction of harmful substances into water bodies and reduce total solids in wastewater. The presence of dyes in water streams has unexceptional effects on living organisms, leading to the need for the eradication of dye molecules from wastewater before discharge. Synthetic organic dyes are considered micropollutants of aquatic ecosystems, and their occurrence in water bodies should be monitored due to their toxicological properties (Tkaczyk, Mitrowska, & Posyniak, 2020).

The removal of BR 46 dye from water is crucial for environmental health and human well-being due to its toxic and colored nature. Contamination of groundwater with colored and toxic wastewater, such as BR 46, can cause environmental problems and negatively impact human health (Abdollahi Ghahi et al., 2022). The worldwide production of colored products and intermediates has led to an increase in liquid effluents containing toxic dyes entering the aquatic environment, making it important to dispose of them (Wiśniewska, Chibowski, Wawrzkiwicz, Onyszko, & Bogatyr, 2022).

BR 46 removal presents specific challenges compared to other dye contaminants (Abdollahi Ghahi et al., 2022). It is a colored and toxic wastewater pollutant that is difficult to remove from water resources. The removal of chemical dyes requires advanced oxidation processes (AOPs) or adsorption techniques (Sharma & Qanungo, 2022). A non-thermal plasma reactor using high-voltage corona discharge has shown 85% degradation efficiency for BR 46 within 30 minutes of treatment time (Abdollahi Ghahi et al., 2022). Another study has explored the use of a carbon and silica-based composite for the removal of BR 46, showing temperature-dependent adsorption capacity (Wiśniewska et al., 2022). The challenges in removing BR 46 include its high toxicity, the presence of azo bonds and associated harmful components, and the difficulty in treating wastewater contaminated with this dye (Saad, Ralha, Abukhadra, Al Zoubi, & Ko, 2023).

Advanced technologies such as nanotechnology and membrane filtration can play a significant role in enhancing the removal efficiency of dyes, a harmful pollutants. Nanofiltration membranes, particularly those incorporating nanocomposite materials like graphene oxide (GO) nanosheets, have shown promising results in terms of higher separation performance and antifouling tendencies. These membranes have increased permeation flux, rejection of Congo Red (CR), and flux recovery ratio, making them effective in removing pollutants from wastewater (Adnan Maykhan, Alsahy, & Bakhtiari, 2023). Additionally, the use of carbon nanomaterials in membrane filtration has also been explored. Carbon nanomaterial-based membranes, such as fullerenes, graphenes, and carbon nanotubes (CNTs),

have high surface areas and can efficiently adsorb pollutants, including dyes, from wastewater (Banjare, Behera, & Banjare, 2023).

Innovative technologies and strategies can be employed to address and prevent such as BR 46 dye contamination in water bodies. One approach is the use of phytoremediation, which involves the use of aquatic plants to filter and immobilize contaminants in water bodies (Agarwal & Rani, 2022). Another strategy is the formation of biofilms, which are aggregates of microbes that can absorb, immobilize, and degrade organic matter in water bodies (Verma, Karande, & Mathur, 2022). AOPs, such as heterogeneous photocatalysis, can also be employed to degrade and mineralize organic compounds in water systems. These processes can be enhanced by the use of carbon-based materials as cocatalysts or support materials for photocatalysts (Sadat et al., 2023).

MXene is a unique and promising material for water purification compared to traditional adsorbents due to its exceptional physicochemical characteristics. These include highly active sites, 2D layered morphology, photocatalytic properties, thermal/electrical conductivity, large inter-layer spacing, superior sorption/reduction capacity, high negative zeta-potential, and the existence of surface functional groups ($-OH$ and $-O$) (Bilal, Khan, & Ihsanullah, 2023). The presence of these functional groups allows for electrostatic attraction and surface complexation mechanisms, enabling the removal of heavy metals from water (Y. Zhang et al., 2023). MXenes also exhibit excellent sorption selectivity, making them effective for removing hazardous contaminants. Furthermore, MXenes can be easily functionalized and tuned to optimize their interlayer spacing, further enhancing their adsorption capabilities (Janjhi et al., 2023). MXenes also offer tunable interlayer spacing and tailorable surface chemistry, making them suitable for a variety of applications in environmental purification (Rana et al., 2023). Additionally, MXene-based adsorbents exhibit ultrahigh adsorption capacity and high stability, making them effective for removing pollutants from wastewater (Qing et al., 2023). MXene-based membranes, adsorbents, and photo-catalysts have been developed for removing antibiotics and heavy metals from water, and they show promise compared to other 2D membranes (Janjhi et al., 2023). Overall, MXene's unique physicochemical properties and its potential for various applications make it a promising material for water purification (Bilal et al., 2023).

The tunability of MXene's surface chemistry allows for the customization of its adsorption capabilities for specific water contaminants. MXenes are two-dimensional materials with unique properties such as high surface area, good thermal stability, and large specific surface area (Gopalram, Kapoor, Kumar, Sunil, & Rangasamy, 2023; Ma et al., 2023; Solangi et al., 2023). The surface reactivity of MXenes depends on the exposed atoms or terminated groups, such as oxygen, fluorine, and chlorine. Different terminations result in different adsorption capacities and oxidation rates for specific contaminants. For example, O-terminated MXene exhibits a significantly higher adsorption capacity and oxidation rate for perfluorooctanoic acid (PFOA) compared to MXenes with F and Cl terminations (Ma et al., 2023). MXenes have demonstrated the capability to adsorb various heavy contaminants, particularly metals such as chromium, copper, lead, and mercury. The adsorption capacity and selectivity of MXene-based adsorbents can be influenced by factors such as water quality, adsorbent quantity, pH, adsorption time, and temperature (Solangi et al., 2023).

MXene plays a significant role in addressing emerging contaminants, including dyes in water sources (Bilal et al., 2023). MXenes have demonstrated the capability to adsorb various heavy contaminants, particularly metals and dyes, from water sources (Pouramini et al., 2023). They have been used as effective adsorbents for the enhanced uptake of different kinds of dyes from aqueous environments (Bilal et al., 2023). MXene-based composite materials have been developed as efficient adsorbents for the removal of pollutants from water, including organic dyes (Pouramini et al., 2023).

$Ti_3C_2T_x$ MXene has been studied for its adsorption efficiency in removing dyes from water. The $Ti_3C_2T_x$ MXene nanofiltration (NF) membrane demonstrated a high rejection rate of 95.44% for CR, a type of azo dye (Li et al., 2023). Additionally, $Ti_3C_2T_x$ MXene showed excellent heavy metal adsorption capacity, including Pb(II) and Cu(II) ions. The delaminated titanium carbide (DL- $Ti_3C_2T_x$) MXene exhibited a higher maximum adsorption capacity for Pb(II) (77.0 mg/g) compared to multilayer (ML- $Ti_3C_2T_x$) MXene (56.68 mg/g). However, the maximum adsorption capacity for Cu(II) was higher in ML- $Ti_3C_2T_x$ (55.46 mg/g) compared to DL- $Ti_3C_2T_x$ (23.08 mg/g) (Y. Zhang et al., 2023).

In terms of sustainability, MXene-based materials offer a promising solution for wastewater treatment, as they can be synthesized from abundant and low-cost precursors. However, the scaling-up process of MXene production is

currently costly, and the applications are still limited. Future research should focus on developing more environmentally friendly synthesis methods and reducing the cost of production to ensure the widespread use of MXene-based materials for water treatment (Tawalbeh et al., 2023).

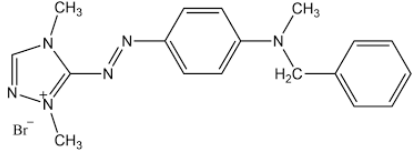
MXene-based materials have been extensively studied for their adsorption efficiency in water treatment applications. However, there is a lack of systematic studies comparing the adsorption efficiency of MXene with other materials specifically for BR 46 removal. While several papers discuss the exceptional physicochemical characteristics of MXenes that make them effective adsorbents for various dyes (Bilal et al., 2023; Li et al., 2023; Qing et al., 2023), including BR 46 (Yan, Liu, Wen, & Liu, 2022), there is no direct comparison with other materials for this specific dye. These studies highlight the potential of MXene-based adsorbents for wastewater treatment and the need for further research to explore their effectiveness in removing BR 46 and other contaminants. The specific aim of this study is to examine the effects of pH, MXene amount, and initial BR 46 concentration on the adsorption of BR 46 from aqueous solutions with $Ti_3C_2T_x$ synthesized by directly etching HF from the MAX phase. The properties of $Ti_3C_2T_x$ were examined using FTIR, XRD, and SEM.

MATERIALS AND METHODS

Materials

Titanium Aluminum Carbide (Ti_3AlC_2 , MAX Phase Micron Powder, APS: 325 Mesh, Purity: 99+ %) was purchased from Nanografi. BR 46 dyestuff was obtained from DyStar and used without purification. The structure and properties of the dyestuff are given in Table 2. HF was obtained from Merck. H_2SO_4 (Sulfuric acid) and NaOH (Sodium hydroxide) were purchased from Merck. Reagent water was produced from a Millipore Milli- Q Ultrapure Gradient 3 V purification system.

Table 1. Properties of the Dyestuff

Chemical Formula	$C_{18}H_{21}BrN_6$
Chemical Structure	
Molecular Weight (g/mol)	401.31
Wavelength Used	534 nm

Characterization Techniques

X-ray diffraction (PANalytical Empyrean XRD, Fourier transform infrared spectroscopy (Jasco FT/IR, 6700, Jasco Inc.), Scanning electron microscope (SEM) (Hitachi SU3500) and UV/Vis spectrometer (PerkinElmer UV/Vis Lambda 365).

Material Synthesis

The Ti_3AlC_2 powder (1 g) was incorporated into 28 mL of a 30% (v/v) HF solution, following a method adapted from the literature (Naguib et al., 2023). Subsequently, the mixture was stirred for 24 hours at 40 °C in a shaking water bath (GFL Shaking Water Bath 1083). The suspension solution underwent multiple washes with deionized water until achieving a neutral pH. Post washes, centrifugation (3 minutes at 4100 rpm) was conducted to isolate the MXene powder after each round of washing with distilled water. This sample was dispersed in 200 mL deionized water and then sonicated (FS-300N Ultrasonic Homogenizer) for 40 min under a nitrogen atmosphere. The solid part was collected by vacuum filtration (membrane pore: 0.22 μm). Finally, the material was dried in a vacuum oven at 60 °C for 24 hours and stored in an environment devoid of light and air.

Material Characterization

XRD patterns were achieved by PANalytical Empyrean XRD at 5 kV voltage and 40 mA current with Cu-K α radiation ($\lambda = 1.5406 \text{ \AA}$) with a 2θ range of 10–90° and used to study the crystal structures of Ti_3AlC_2 MAX phase and $Ti_3C_2T_x$ MXene phase. FTIR spectra of before and after adsorption MXene material were recorded on Jasco

FT/IR, 6700. The SEM images were carried out using the SEM (Hitachi SU3500). The absorbance values of the liquid samples were read using the UV/Vis spectrophotometer (PerkinElmer UV/Vis Lambda 365) device and the dye concentrations were calculated using the previously prepared calibration curve.

Adsorption Experiment

In experimental studies on batch adsorption, the impact of the initial pH of the solution, the quantity of adsorbent, and the initial concentration of dye on the efficiency of removing BR 46 dyestuff were analyzed. The dye solutions utilized in the experimental series were created at the desired concentrations through dilution of a stock solution. Following the adjustment of pH levels in the prepared dye solutions, specific quantities of adsorbent were introduced to the solutions and placed in an orbital shaker apparatus (Gallenkamp) at a consistent temperature, agitated at 180 rpm. Samples were extracted at set intervals and centrifuged utilizing a centrifuge apparatus (Nüve 400 NF) at 4100 rpm for 2 minutes to segregate the solid and liquid components. The absorbance readings of the liquid samples were measured using a UV/Vis spectrophotometer device, and dye concentrations were determined by referencing a previously established calibration curve. The initial phase of the adsorption experiments involved the investigation of the impact of pH on dye removal across various pH levels while maintaining other variables constant. The pH of the solutions was adjusted to the desired levels using dilute solutions of H₂SO₄ and NaOH. Subsequently, the influence of varying amounts of adsorbent was explored to understand its effect. The impact of the initial dye concentration on removal efficiency was assessed at different concentrations within the range of 25-125 mg/L. The relative calculation formula of the removal rate-R (%) (Eq.1) is as follows:

$$R(\%) = 100 \times \frac{C_0 - C_t}{C_0} \quad (1)$$

Where C_0 (mg/L) and C_t (mg/L) are the initial concentration of the solution (mg/L) and the concentration of the solution at time t .

RESULTS AND DISCUSSION

Characterization

Using an XRD pattern, the structural properties of Ti₃C₂T_x MXene and MAX precursor were examined (Figure 1). Ti₃AlC₂'s strongest peak is located in the 104 plane at $2\theta = 38.69^\circ$. After etching with 30% (v/v) HF after 24 hours at 40°C, the strongest signals of the MAX precursor at 38.69° vanish, indicating that the Al layers are nearly etched away (G. Zhang et al., 2020). The characteristic peaks (Figure 1) of Ti₃C₂T_x at $2\theta = 28.58^\circ$ and 60.78° correspond to (0 0 6) and (1 1 0) planes of Ti₃C₂T_x, respectively (Y. Wang et al., 2019).

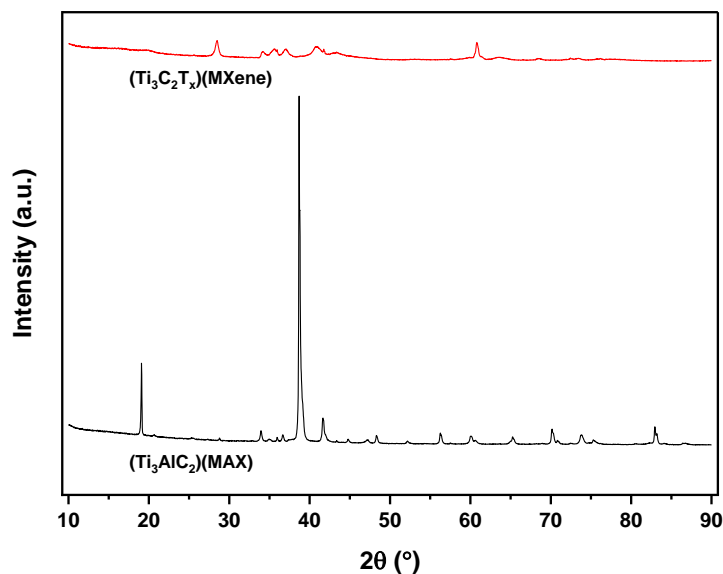


Figure 1. XRD Patterns of Ti₃AlC₂, and Ti₃C₂T_x

Figure 2 (a) and (b) show the SEM images of the synthesized $Ti_3C_2T_x$ before and after adsorption, respectively. Specifically, Figure 2 (a) and (b) display a distinct accordion-like multilayer structure, which is the result of the etching of the A-layer and the breakdown of the weak M-A bond in the MAX phase (R. Wang et al., 2023). As shown in Figure 2 (b), it can be seen that BR 46 molecules enter between $Ti_3C_2T_x$ interlayers after the adsorption process. The presence of these interlayer gaps in the MXene structure provided a good opportunity for BR 46 adsorption.

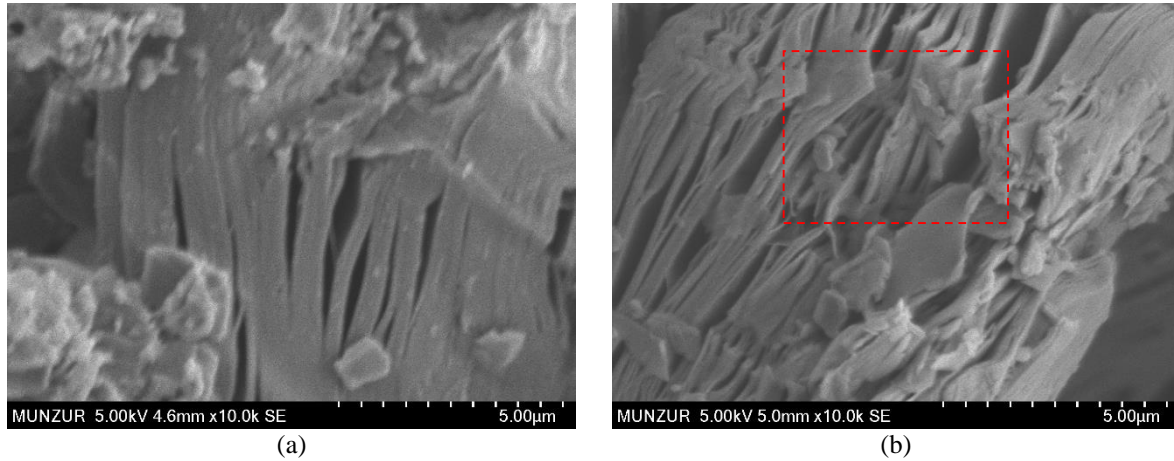


Figure 2. SEM Images of (a) $Ti_3C_2T_x$ Before Adsorption, and (b) $Ti_3C_2T_x$ After Adsorption

Figure 3 illustrates the FTIR spectra of $Ti_3C_2T_x$ before and after BR 46 adsorption. The peaks in the band gap $2365-2309\text{ cm}^{-1}$, the peaks around 2100 cm^{-1} , and the peaks at 1010 and 1021 cm^{-1} correspond to strong $O=C=O$ stretching, weak $C\equiv C$ stretching, and strong $C-F$ stretching, respectively. After adsorption, a new peak appeared at 678 cm^{-1} , which could be attributed to the strong stretching of $C-Br$. The appearance of a new peak suggests the formation of the chemical bond occurred between the material and BR 46 molecules due to the adsorption.

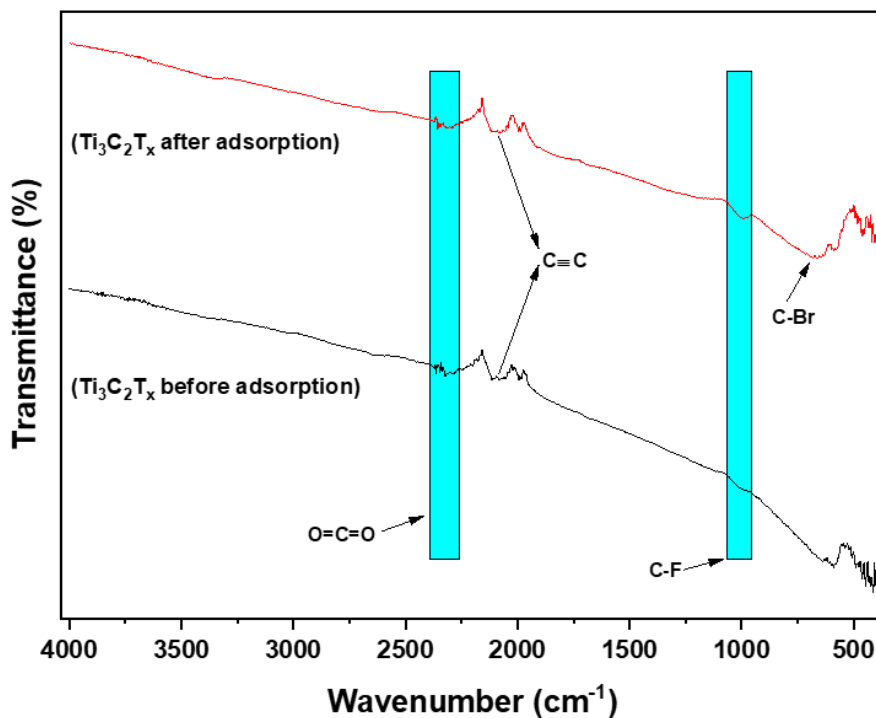


Figure 3. The FTIR Spectra of $Ti_3C_2T_x$ Before and After BR 46 Adsorption

Effect of pH

Figure 4 shows the effect of different pH levels (2, 4, 7, 9, 11) on the removal efficiency of BR 46 over time. The removal efficiency is highest at pH 2 and decreases with increasing pH values. Higher removal efficiency at pH 2 suggests that $Ti_3C_2T_x$ has a higher affinity for BR 46 in acidic conditions. This could be due to the protonation of the adsorbent surface, increasing the positive charge and enhancing the electrostatic attraction between the negatively charged dye molecules and the positively charged surface sites (Obayomi et al., 2024). Lower removal efficiency at higher pH levels (7, 9, 11) indicates reduced adsorption. At higher pH, the surface of $Ti_3C_2T_x$ might be negatively charged due to deprotonation, leading to repulsion between the negatively charged dye molecules and the adsorbent surface (Aguiar et al., 2014). pH 2 was chosen for subsequent experiments because it resulted in the highest adsorption efficiency for BR 46, as indicated by Figure 4 showing maximum removal at this pH level.

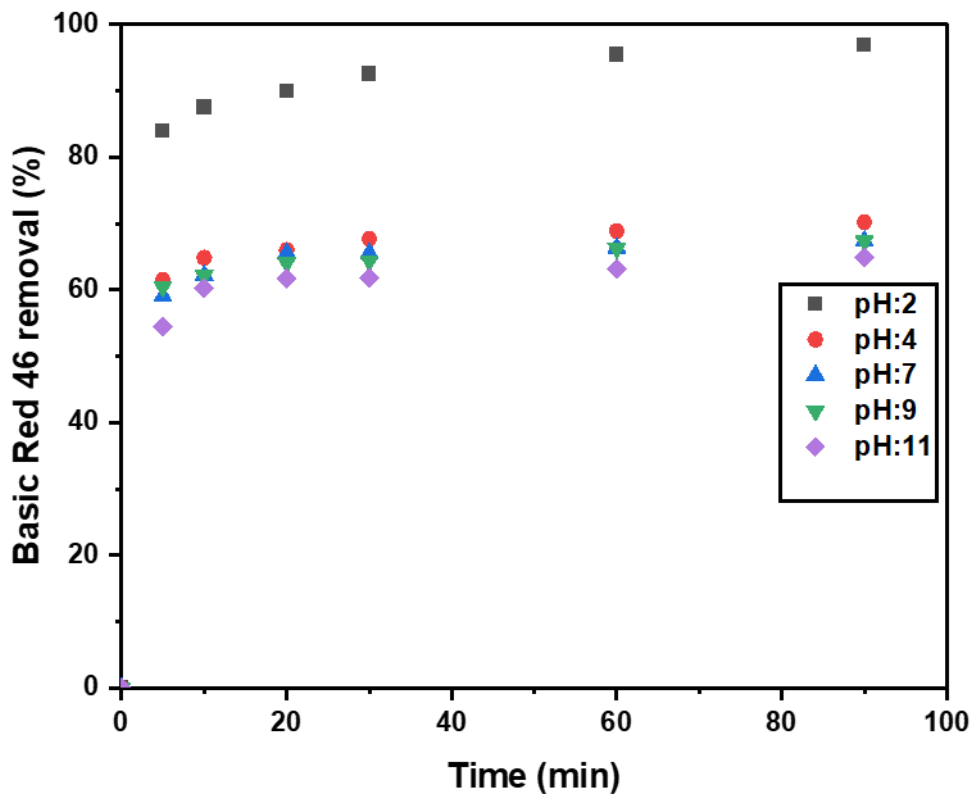


Figure 4. Effect of the Solution pH on BR 46 Adsorption by $Ti_3C_2T_x$ (Initial BR 46 Concentration: 50 mg/L; MXene Amount: 2 g/L; Temperature: 25 °C)

Effect of MXene Amount

Figure 5 shows the removal efficiency of BR 46 over time at different MXene concentrations (1 g/L, 2 g/L, 4 g/L, 6 g/L, 8 g/L). The efficiency increases with the amount of MXene up to 4 g/L and remains constant thereafter. The optimum amount of MXene for maximum adsorption efficiency is 4 g/L. In addition, it is seen that the removal efficiency increases rapidly in the first 20-30 minutes and then gradually stabilizes. An increase in the amount of MXene above 4 g/L did not significantly increase the adsorption efficiency. The plateau indicates that all available adsorption sites are saturated at 4 g/L and that additional MXene does not provide a more effective surface area for adsorption (Ghorbani, Eisazadeh, & Ghoreyshi, 2012). Subsequent experiments were carried out with an amount of 4 g/L MXene as it ensured maximum adsorption efficiency without wasting additional material.

Effect of Initial BR 46 Concentration

Figure 6 illustrates the effect of varying initial BR 46 concentrations (25 mg/L, 50 mg/L, 75 mg/L, 100 mg/L, 125 mg/L) on removal efficiency over time. Table 2 summarizes the adsorption efficiencies and equilibrium uptake

capacities. Conditions were maintained constant during experiments at a pH of 2, an MXene amount of 4 g/L, and a temperature of 25 °C. Higher initial BR 46 concentrations result in lower removal efficiency due to the limited availability of adsorption sites (Wong et al., 2020). Higher initial concentrations result in higher adsorption capacities due to greater availability of dye molecules, which saturate the adsorbent more quickly.

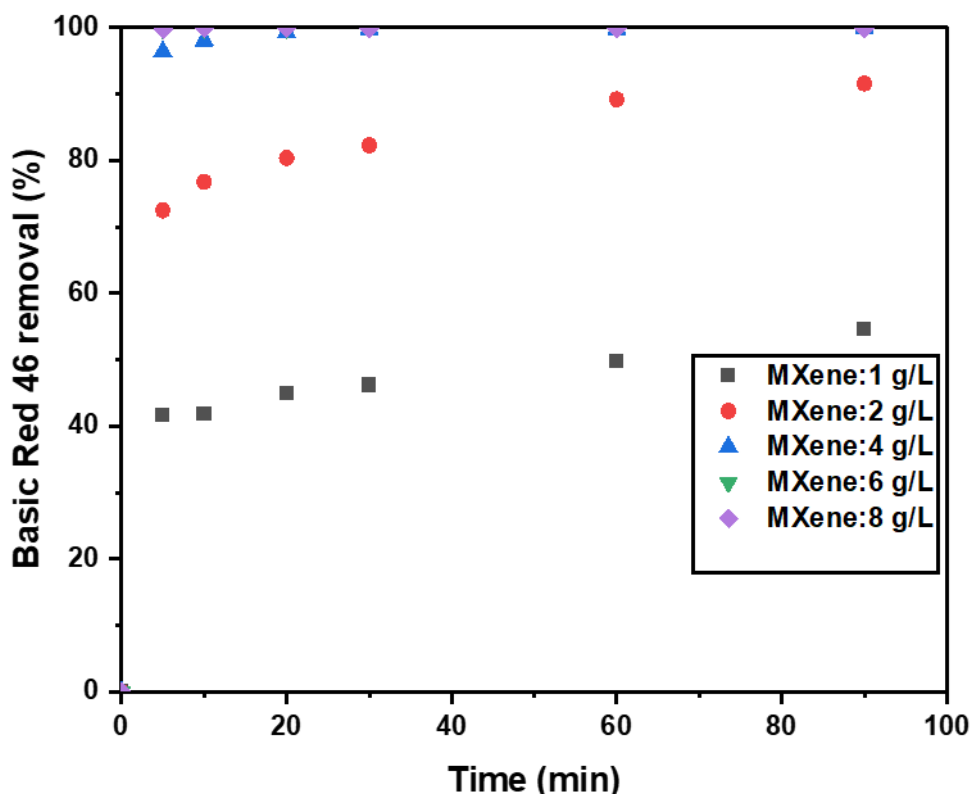


Figure 5. Effect of the MXene Amount on BR 46 Adsorption by $Ti_3C_2T_x$ (Initial BR 46 Concentration: 50 mg/L; pH: 2; Temperature: 25 °C)

Table 2. The Equilibrium Uptake Capacities and Adsorption Efficiencies Obtained at Different Initial BR 46 Concentrations

C_0 mg/L	q_e mg/g	Adsorption (%)
25	6.25	99.96
50	12.48	99.8
75	12.75	68
100	15.93	63.7
125	21.28	68.08

CONCLUSIONS

This study successfully demonstrates the potential of $Ti_3C_2T_x$ MXene as an effective adsorbent for the removal of BR 46 dye from aqueous solutions. The adsorption efficiency was significantly influenced by pH, with acidic conditions (pH 2). XRD analysis confirmed the successful etching of Ti_3AlC_2 to $Ti_3C_2T_x$, indicated by the disappearance of the Al layers. SEM images revealed an accordion-like multilayer structure of $Ti_3C_2T_x$, which facilitated the intercalation of BR 46 molecules. FTIR spectra showed the formation of new peak post-adsorption, suggesting chemical interactions between $Ti_3C_2T_x$ and BR 46 molecules, enhancing the adsorption process. The adsorption efficiency increased with the amount of $Ti_3C_2T_x$ up to 4 g/L. The higher initial concentrations of BR 46 led to greater adsorption capacities, they also resulted in lower removal efficiencies due to the finite number of adsorption sites on the MXene surface. These findings underscore the efficacy of $Ti_3C_2T_x$ MXene as a high-

performance adsorbent for BR 46 removal, offering a promising solution for dye contamination in water treatment applications.

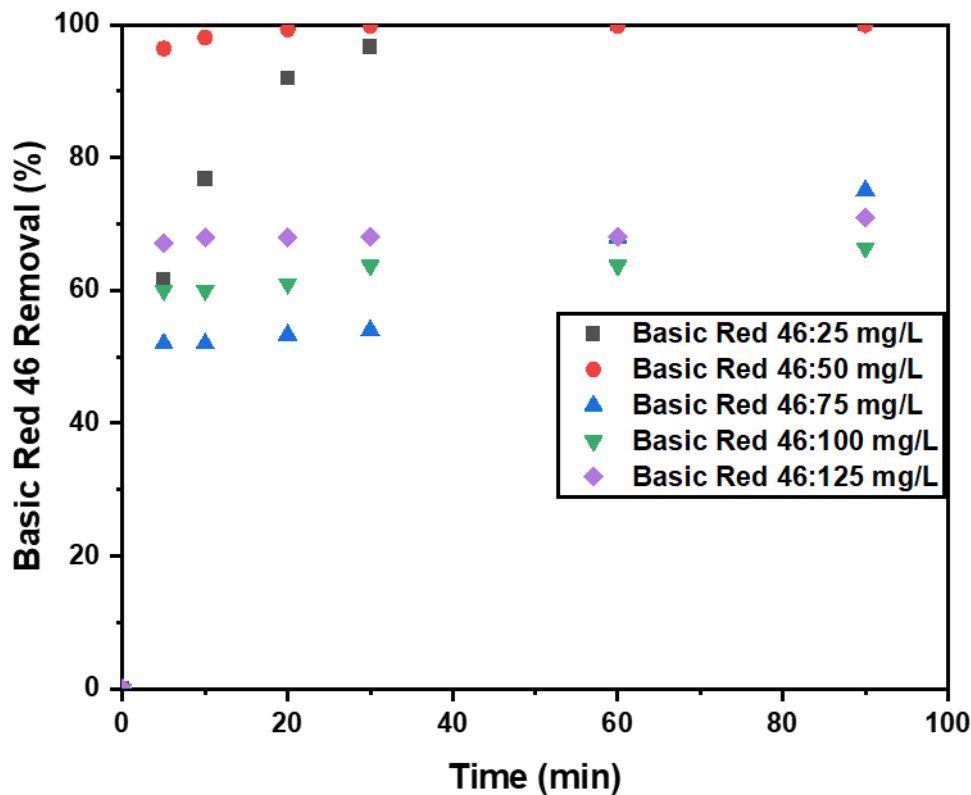


Figure 6. Effect of Initial BR 46 Concentration on BR 46 Adsorption by $Ti_3C_2T_x$ (MXene Amount: 4 g/L; pH: 2; Temperature: 25 °C)

REFERENCES

- Abdollahi Ghahi, N., Nohekhan, M., Rezazadeh Azari, F., Rezaei Fard, B., Bakhtiari Ramezani, M., Beigmohammadi, N., ... Abdollahi Dargah, M. (2022). Degradation of basic red 46 dye from color wastewater using cold atmospheric plasma. *Journal of Nuclear Research and Applications*, 2(4), 21–24. <https://doi.org/https://doi.org/10.24200/jon.2022.1029>
- Adnan Maykhan, N., Alsahy, Q. F., & Bakhtiari, O. (2023). Incorporation of graphene oxide nanosheets into polyethersulfone membranes to improve their separation performance and antifouling characteristics for Congo red removal. *Water Environment Research*, 95(5), e10866. <https://doi.org/https://doi.org/10.1002/wer.10866>
- Agarwal, P., & Rani, R. (2022). Strategic management of contaminated water bodies: Omics, genome-editing and other recent advances in phytoremediation. *Environmental Technology & Innovation*, 27, 102463. <https://doi.org/https://doi.org/10.1016/j.eti.2022.102463>
- Aguiar, J. E., Bezerra, B. T. C., Siqueira, A. C. A., Barrera, D., Sapag, K., Azevedo, D. C. S., ... Silva Jr, I. J. (2014). Improvement in the adsorption of anionic and cationic dyes from aqueous solutions: A comparative study using aluminium pillared clays and activated carbon. *Separation Science and Technology*, 49(5), 741–751. <https://doi.org/https://doi.org/10.1080/01496395.2013.862720>
- Allirani, S. (2022). Smart and Secure Dyeing Industrial Water Pollution Monitoring Using IoT. *International Journal of Hyperconnectivity and the Internet of Things (IJHIoT)*, 6(1), 1–5. <https://doi.org/https://doi.org/10.4018/ijhiot.305227>
- Banjare, M. K., Behera, K., & Banjare, R. K. (2023). Carbon Allotropes in Other Metals (Cu, Zn, Fe etc.) Removal.

- Carbon Allotropes and Composites: Materials for Environment Protection and Remediation*, 113–154. <https://doi.org/https://doi.org/10.1002/9781394167913.ch7>
- Bilal, M., Khan, U., & Ihsanullah, I. (2023). MXenes: The Emerging Adsorbents for the Removal of Dyes from Water. *Journal of Molecular Liquids*, 122377. <https://doi.org/https://doi.org/10.1016/j.molliq.2023.122377>
- Devasia, S., Anand, S., & Nair, A. J. (2022). Laccase mediated bioremediation of industrial dyes by a potent strain of *Arthrographis* sp. *International Journal of Environment and Waste Management*, 29(3), 278–290. <https://doi.org/https://doi.org/10.1504/ijewm.2022.122679>
- Ghorbani, M., Eisazadeh, H., & Ghoreyshi, A. A. (2012). Removal of zinc ions from aqueous solution using polyaniline nanocomposite coated on rice husk. *Iranica Journal of Energy & Environment*, 3(1). <https://doi.org/https://doi.org/10.5829/idosi.ijee.2012.03.01.3343>
- Ghosh, S., & Sarkar, B. (2022). Emerging dye contaminants of industrial origin and their enzyme-assisted biodegradation. In *Biodegradation and Detoxification of Micropollutants in Industrial Wastewater* (pp. 79–102). Elsevier. <https://doi.org/https://doi.org/10.1016/b978-0-323-88507-2.00005-1>
- Gopalram, K., Kapoor, A., Kumar, P. S., Sunil, A., & Rangasamy, G. (2023). MXenes and MXene-Based Materials for Removal and Detection of Water Contaminants: A Review. *Industrial & Engineering Chemistry Research*, 62(17), 6559–6583. <https://doi.org/https://doi.org/10.1021/acs.iecr.3c00595>
- Hashemi, S. H., & Kaykhahi, M. (2022). Azo dyes: sources, occurrence, toxicity, sampling, analysis, and their removal methods. In *Emerging freshwater pollutants* (pp. 267–287). Elsevier. <https://doi.org/https://doi.org/10.1016/b978-0-12-822850-0.00013-2>
- Janjhi, F. A., Ihsanullah, I., Bilal, M., Castro-Muñoz, R., Boczkaj, G., & Gallucci, F. (2023). MXene-based materials for removal of antibiotics and heavy metals from wastewater—A review. *Water Resources and Industry*, 100202. <https://doi.org/https://doi.org/10.1016/j.wri.2023.100202>
- Kamsonlian, S., & Agarwal, V. (2023). Review on synthesis of plant-mediated green iron nanoparticles and their application for decolorization of dyes. *Materials Today: Proceedings*, 78, 99–107. <https://doi.org/https://doi.org/10.1016/j.matpr.2022.11.308>
- Lekhakh, U. M. (2023). Ecotoxicity of synthetic dyes. In *Current Developments in Bioengineering and Biotechnology* (pp. 45–67). Elsevier. <https://doi.org/https://doi.org/10.1016/b978-0-323-91235-8.00021-8>
- Li, Y., Luo, H., Ji, W., Li, S., Nian, P., Xu, N., ... Wei, Y. (2023). Visible-light-driven photocatalytic ZnO@Ti₃C₂T_x MXene nanofiltration membranes for enhanced organic dyes removal. *Separation and Purification Technology*, 124420. <https://doi.org/https://doi.org/10.1016/j.seppur.2023.124420>
- Ma, Q., Gao, J., Moussa, B., Young, J., Zhao, M., & Zhang, W. (2023). Electrosorption, Desorption, and Oxidation of Perfluoroalkyl Carboxylic Acids (PFCAs) via MXene-Based Electrocatalytic Membranes. *ACS Applied Materials & Interfaces*. <https://doi.org/https://doi.org/10.1021/acsami.3c03991>
- Maheshwari, K., Agrawal, M., & Gupta, A. B. (2021). Dye pollution in water and wastewater. *Novel Materials for Dye-Containing Wastewater Treatment*, 1–25. https://doi.org/https://doi.org/10.1007/978-981-16-2892-4_1
- Mustafa, S., Jamil, K., Zhang, L., & Girmay, M. B. (2022). Does Public Awareness Matter to Achieve the UN's Sustainable Development Goal 6: Clean Water for Everyone? *Journal of Environmental and Public Health*, 2022. <https://doi.org/https://doi.org/10.1155/2022/8445890>
- Naguib, M., Kurtoglu, M., Presser, V., Lu, J., Niu, J., Heon, M., ... Barsoum, M. W. (2023). Two-dimensional nanocrystals produced by exfoliation of Ti₃AlC₂. In *MXenes* (pp. 15–29). Jenny Stanford Publishing. <https://doi.org/https://dx.doi.org/10.1201/9781003306511-4>
- Obayomi, K. S., Lau, S. Y., Danquah, M. K., Zhang, J., Chiong, T., Obayomi, O. V., ... Rahman, M. M. (2024). A response surface methodology approach for the removal of methylene blue dye from wastewater using sustainable and cost-effective adsorbent. *Process Safety and Environmental Protection*. <https://doi.org/https://doi.org/10.1016/j.psep.2024.01.106>
- Pouramini, Z., Mousavi, S. M., Babapoor, A., Hashemi, S. A., Pynadathu Rumjit, N., Garg, S., ... Chiang, W.-H. (2023). Recent Advances in MXene-Based Nanocomposites for Wastewater Purification and Water Treatment: A Review. *Water*, 15(7), 1267. <https://doi.org/https://doi.org/10.3390/w15071267>

- Qing, Q., Shi, X., Hu, S., Li, L., Huang, T., Zhang, N., & Wang, Y. (2023). Synchronously Enhanced Removal Ability and Stability of MXene through Biomimetic Modification. *Langmuir*, 39(27), 9453–9467. <https://doi.org/10.1021/acs.langmuir.3c00987>
- Rana, G., Dhiman, P., Kumar, A., Sharma, G., Verma, Y., & Chauhan, A. (2023). Functionalization of two-dimensional MXene-based nanomaterials for water purifications and energy conversion applications: A review. *Materials Science in Semiconductor Processing*, 165, 107645. <https://doi.org/https://doi.org/10.1016/j.mssp.2023.107645>
- Saad, I., Ralha, N., Abukhadra, M. R., Al Zoubi, W., & Ko, Y. G. (2023). Recent advances in photocatalytic oxidation techniques for decontamination of water. *Journal of Water Process Engineering*, 52, 103572. <https://doi.org/https://doi.org/10.1016/j.jwpe.2023.103572>
- Sadat, H., Guettai, N., Berkani, M., Hoang, H. Y., Shanmuganathan, R., Pugazhendhi, A., & Kadmi, Y. (2023). Recent advances in photochemical-based nanomaterial processes for mitigation of emerging contaminants from aqueous solutions. *Applied Nanoscience*, 13(6), 3905–3924. <https://doi.org/https://doi.org/10.1007/s13204-022-02627-y>
- Sharma, P., & Qanungo, K. (2022). Challenges in Effluents Treatment Containing Dyes. *Adv Res Text Eng*, 7(2), 1075. <https://doi.org/https://doi.org/10.26420/advrestexteng.2022.1075>
- Solangi, N. H., Karri, R. R., Mubarak, N. M., Mazari, S. A., Jatoi, A. S., & Koduru, J. R. (2023). Emerging 2D MXene-based adsorbents for hazardous pollutants removal. *Desalination*, 549, 116314. <https://doi.org/https://doi.org/10.1016/j.desal.2022.116314>
- Tawalbeh, M., Mohammed, S., Al-Othman, A., Yusuf, M., Mofijur, M., & Kamyab, H. (2023). MXenes and MXene-based materials for removal of pharmaceutical compounds from wastewater: Critical review. *Environmental Research*, 115919. <https://doi.org/https://doi.org/10.1016/j.envres.2023.115919>
- Tkaczyk, A., Mitrowska, K., & Posyniak, A. (2020). Synthetic organic dyes as contaminants of the aquatic environment and their implications for ecosystems: A review. *Science of the Total Environment*, 717, 137222. <https://doi.org/https://doi.org/10.1016/j.scitotenv.2020.137222>
- Verma, A. K., Karande, S., & Mathur, A. (2022). Role of biofilms to curb contamination in water bodies. In *Relationship Between Microbes and the Environment for Sustainable Ecosystem Services, Volume 2* (pp. 77–93). Elsevier. <https://doi.org/https://doi.org/10.1016/b978-0-323-89937-6.00006-1>
- Wang, R., Cao, H., Yao, C., Peng, C., Qiu, J., Dou, K., ... Wang, W. (2023). Construction of alkalinized MXene-supported CoFe₂O₄/CS composites with super-strong adsorption capacity to remove toxic dyes from aqueous solution. *Applied Surface Science*, 624, 157091. <https://doi.org/https://doi.org/10.1016/j.apsusc.2023.157091>
- Wang, Y., Gao, X., Zhang, L., Wu, X., Wang, Q., Luo, C., & Wu, G. (2019). Synthesis of Ti₃C₂/Fe₃O₄/PANI hierarchical architecture composite as an efficient wide-band electromagnetic absorber. *Applied Surface Science*, 480, 830–838. <https://doi.org/https://doi.org/10.1016/j.apsusc.2019.03.049>
- Wiśniewska, M., Chibowski, S., Wawrzkiwicz, M., Onyszko, M., & Bogatyrov, V. (2022). CI Basic Red 46 removal from sewage by carbon and silica based composite: equilibrium, kinetic and electrokinetic studies. *Molecules*, 27(3), 1043. <https://doi.org/https://doi.org/10.3390/molecules27031043>
- Wong, S., Ghafar, N. A., Ngadi, N., Razmi, F. A., Inuwa, I. M., Mat, R., & Amin, N. A. S. (2020). Effective removal of anionic textile dyes using adsorbent synthesized from coffee waste. *Scientific Reports*, 10(1), 2928. <https://doi.org/https://doi.org/10.1038/s41598-020-60021-6>
- Yan, J., Liu, P. F., Wen, H. X., & Liu, H. J. (2022). Effective Removal of Basic Red 46 with Ti₃C₂ Powder Modified with Citric acid. *ChemistrySelect*, 7(29), e202201733. <https://doi.org/https://doi.org/10.1002/slct.202201733>
- Zhang, G., Wang, T., Xu, Z., Liu, M., Shen, C., & Meng, Q. (2020). Synthesis of amino-functionalized Ti₃C₂T_x MXene by alkalization-grafting modification for efficient lead adsorption. *Chemical Communications*, 56(76), 11283–11286. <https://doi.org/https://doi.org/10.1039/d0cc04265j>
- Zhang, Y., Luo, J., Feng, B., Xu, H., Sun, Y., Gu, X., ... Ren, H. (2023). Delamination of multilayer Ti₃C₂T_x MXene alters its adsorption and reduction of heavy metals in water. *Environmental Pollution*, 330, 121777. <https://doi.org/https://doi.org/10.1016/j.envpol.2023.121777>